

# Unidirectional emission from a cardioid-shaped microcavity laser

In-Goo Lee,<sup>1</sup> Sung-Min Go,<sup>1</sup> Jin-Hyeok Ryu,<sup>1</sup> Chang-Hwan Yi,<sup>2</sup>  
Sung-Bock Kim,<sup>3</sup> Kwang Ryung Oh,<sup>3</sup> and Chil-Min Kim<sup>2,\*</sup>

<sup>1</sup>Department of Physics, Sogang University, Seoul 121-742, South Korea

<sup>2</sup>Department of Emerging Materials Science, DGIST, Hyeonpungmyeon, Daegu, 711-873, South Korea

<sup>3</sup>IT Convergence and Components Lab. ETRI, Yusong-Gu, Daejeon 305-700, South Korea

\*[chmkim@dgist.ac.kr](mailto:chmkim@dgist.ac.kr)

**Abstract:** We find unidirectional emission in a cardioid-shaped microcavity laser. When a deformation parameter is well adjusted, rays starting around a period-5 unstable periodic orbit emit unidirectionally. To confirm the emission direction, we fabricate a laser by using an InGaAsP semiconductor and investigate emission characteristics. When the laser is excited by current injection with a dc current, resonances localized on the period-5 unstable periodic orbit emit unidirectionally.

© 2016 Optical Society of America

**OCIS codes:** (140.3945) Microcavities; (140.5960) Semiconductor lasers; (140.3948) Microcavity devices.

---

## References and links

1. J. U. Nöckel and A. D. Stone, "Ray and wave chaos in asymmetric resonant optical cavities," *Nature* **385**, 45–47 (1997).
2. C. Gmachl, F. Capasso, E. E. Narimanov, J. U. Nöckel, A. D. Stone, J. Faist, D. L. Sivco, and A. Y. Cho, "High-Power Directional Emission from Microlasers with Chaotic Resonators," *Science* **280**, 1556–1564 (1998).
3. T. Harayama and S. Shinohara, "Two-Dimensional Microcavity Laser," *Laser Photonics Rev.* **5**, 247–271 (2011).
4. H. Cao and J. Wiersig, "Dielectric Microcavities: Model Systems for Wave Chaos and Non-Hermitian Physics," *Rev. Mod. Phys.* **87**, 61–111 (2015).
5. G. D. Chern, H. E. Tureci, A. D. Stone, R. K. Chang, M. Kneissl, and N. M. Johnson, "Unidirectional lasing from InGaN multiple-quantum-well spiral-shaped micropillars," *Appl. Phys. Lett.* **83**, 1710–1712 (2003).
6. C. M. Kim, J. Cho, J. Lee, S. Rim, S. H. Lee, K. R. Oh, and J. H. Kim, "Continuous Wave Operation of a Spiral-Shaped Microcavity Laser," *Appl. Phys. Lett.* **92**, 131110 (2008).
7. J. Wiersig and M. Hentschel, "Combining Directional Light Output and Ultralow Loss in Deformed Microdisks," *Phys. Rev. Lett.* **100**, 033901 (2008).
8. C. H. Yi, M. W. Kim, and C. M. Kim, "Lasing Characteristics of a Limaçon-Shaped Microcavity Laser," *Appl. Phys. Lett.* **95**, 141107 (2009).
9. C. L. Yan, Q. J. Wang, L. Diehl, M. Hentschel, J. Wiersig, N. Yu, C. Pflügl, F. Capasso, M. A. Belkin, T. Edamura, M. Yamanishi, and H. Kan, "Directional emission and universal far-field behavior from semiconductor lasers with limaçon-shaped microcavity," *Appl. Phys. Lett.* **94**, 251101 (2009).
10. Q. H. Song, L. Ge, A. D. Stone, H. Cao, J. Wiersig, J.-B. Shim, J. Unterhinninghofen, W. Fang, and G. S. Solomon, "Directional Laser Emission from a Wavelength-Scale Chaotic Microcavity," *Phys. Rev. Lett.* **105**, 103902 (2010).
11. C. L. Zou, F.-W. Sun, C.-H. Dong, X.-W. Wu, J.-M. Cui, Y. Yang, G.-C. Guo, and Z.-F. Han, "Mechanism of unidirectional emission of ultrahigh Q whispering gallery mode in microcavities," arXiv:0908.3531v1 (2008).
12. M. S. Kurdoglyan, S.-Y. Lee, S. Rim, and C.-M. Kim, "Unidirectional lasing from a microcavity with a rounded isosceles triangle shape," *Opt. Lett.* **29**, 2758–2760 (2004).
13. J. Ryu and M. Hentschel, "Designing coupled microcavity lasers for high-Q modes with unidirectional light emission," *Opt. Lett.* **36**, 1116–1118 (2011).
14. J. H. Lee, S. Rim, J. H. Cho, C. M. Kim, "Unidirectional resonance modes supported by secondary islands in a microcavity comprised of two half-ellipses," *Phys. Rev. A* **83**, 033815 (2011).

15. Q. J. Wang, C. Yan, N. Yu, J. Unterhinninghofen, J. Wiersig, C. Pflügl, L. Diehl, T. Edamura, M. Yamanishi, H. Kan, and F. Capasso, "Whispering-gallery mode resonators for highly unidirectional laser action," *Proc. Natl. Acad. Sci. U. S. A.* **107**(52), 22407–22412 (2010).
16. A. Bäcker, F. Steiner and P. Stifter, "Spectral statistics in the quantized cardioid billiard," *Phys. Rev. E.* **52**, 2463 (1995).
17. H. Bruss and N. D. Whelan, "Edge diffraction, trace formulae and the cardioid billiard," *Nonlinearity.* **9**, 1023 (1996).
18. A. Bäcker and H. R. Dullin, "Symbolic dynamics and periodic orbits for the cardioid billiard," *J. Phys. A: Math. Gen.* **30**, 6 (1997).
19. C. H. Yi, M. W. Kim and C. M. Kim, "Lasing characteristics of a limaçon-shaped microcavity laser," *Appl. Phys. Lett.* **95**, 141107 (2009).
20. R. Polson, G. Levina, and Z. Vardeny, "Spectral analysis of polymer microring lasers," *Appl. Phys. Lett.* **36**, 3658 (2000).
21. T. Ben-Messaoud and J. Zyss, "Unidirectional laser emission from polymer-based spiral microdisks," *Appl. Phys. Lett.* **86**(24), 241110 (2005).
22. C. H. Yi, S. H. Lee, M. W. Kim, J. Cho, J. Lee, S. Y. Lee, J. Wiersig and C. M. Kim, "Light emission of a scarlike mode with assistance of quasiperiodicity," *Phys. Rev. A* **84**, 041803(R) (2011).

## 1. Introduction

Since the report on directional emission in chaotic microcavity [1, 2], microcavities of various shapes have been extensively studied to obtain better emission direction [3, 4]. When the emission direction of a microcavity is unidirectional, coupling with a fiber or a waveguide becomes much easier using conventional techniques. These microcavity lasers of varying shapes, which emit unidirectionally, have been continually developed for application as an optical source in optoelectronic circuits. Thus far, a spiral [5, 6], a limaçon [7–10], a gibbous [11], a rounded isosceles triangular [12] and a coupled microcavity [13], microcavity comprising a half-circle and a half-ellipse [14], and elliptic microcavity with a notch [15] have been reported for unidirectional emission. These are lasers deformed from a circle, and therefore, the operating characteristics are based on the quantum chaos theory.

Because most of these lasers have reflection symmetry, lasing modes are emitted out through two emission windows owing to the clockwise (CW) and the counter-clockwise (CCW) traveling waves. When the emission directions of the CW and the CCW traveling waves are the same, emission is unidirectional. Based on this, we demonstrate that when a deformation parameter is well adjusted, a chaotic microcavity laser with reflection symmetry can emit unidirectionally despite two emission windows. To show the characteristics of this unidirectional emission in a microcavity with reflection symmetry, we investigate the emission characteristics of a cardioid-shaped microcavity laser, where no laser emission has been observed till date.

The cardioid shape is given as follows:

$$R = R_0 \left( 1 + \varepsilon \cos \frac{\theta}{2} \right) \quad (-\pi < \theta < \pi) \quad (1)$$

where  $\varepsilon$  is the deformation parameter,  $\theta$  is the angle from the  $x$ -axis, and  $R_0$  is the radius at  $\theta = \pm\pi$ . The cavity has a cusp because of the cosine term, which results in fully chaotic behaviors in classical dynamics. In this microcavity, various chaotic properties have been investigated in relation with quantum chaos theory [16–18].

## 2. Ray dynamical analysis

First, we analyze the emission directions of a transverse electric (TE) polarized wave depending on the deformation parameter using ray dynamics for an effective refractive index of  $n_e = 3.3$ , whose conditions coincide with those of fabricated InGaAsP semiconductor lasers. In ray dynamical analysis, we find highly unidirectional emission at  $\varepsilon = 0.48$ , as shown in Fig. 1(a),

which are rays emitting from the cavity. Although the CW and the CCW traveling rays emit through different emission windows, their directions are the same. In the main emissions, there are still weak backward emissions around the cusp. Figure 1(b) shows an angularly distributed far-field pattern (FFP), which is obtained at a distance of  $\frac{50}{3}R_0$ . As shown in the figure, the main emission intensity is approximately eight times higher than that of other directions.

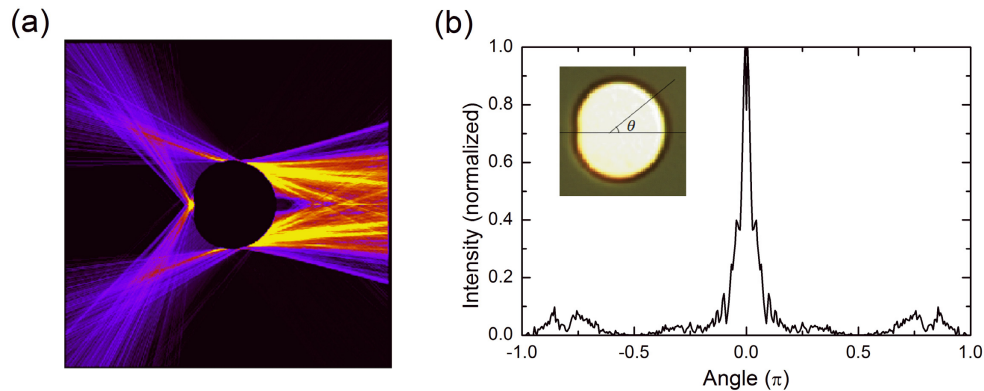


Fig. 1. Unidirectional emission of a cardioid-shaped microcavity at  $\varepsilon = 0.48$ , obtained by ray dynamics. (a) Emission of rays outside the cavity and (b) FFP.

The periodic orbit supporting the emission direction is obtained by backward calculation from the emission. Figure 2(a) shows the periodic orbit and the trajectory of a ray originating from the orbit in the microcavity. A pentagon-type orbit marked by a yellow line is the periodic orbit. A ray originating from around the orbit emits as shown by the red trajectory after bouncing off the cavity boundary several times. Figure 2(b) shows the survival probability distribution (SPD) on the Birkhoff coordinates. In the figure, we can observe several tongues below the critical line that indicate emission. The blue circles on the SPD are the pentagon type orbits. Because of reflection symmetry, only the CCW direction is present. When the rays originate from the periodic orbit, they follow the unstable manifold embedded in the chaotic

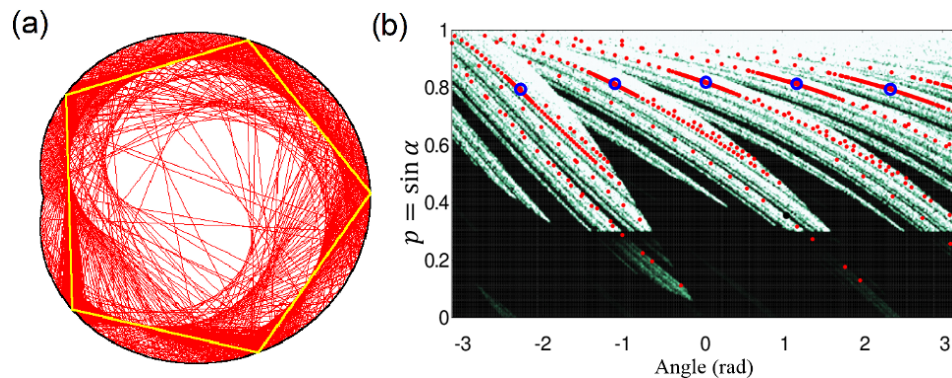


Fig. 2. Ray dynamics and SPD. (a) Ray dynamics in the cardioid microcavity. The yellow pentagon is the period-5 unstable periodic orbit. (b) SPD. The blue circles are the period-5 periodic orbits and the red dots are the trajectories of rays originating around the period-5 periodic orbit. We consider CCW traveling rays because of reflection symmetry of the microcavity.

sea as marked by the red dots on the SPD. After 100 iterations, the rays reach the tongues below the critical line. This is the emission of the rays, which originate from the pentagon-type orbit. From the trajectory in the microcavity and the SPD, we can confirm the periodic orbit supporting the emission directions.

### 3. Experimental results

For experimental verification, we fabricated a microcavity laser using an InGaAsP semiconductor with an effective refractive index of  $n_e \sim 3.3$ . The fabrication process is the same as in [19]. The fabricated laser is shown as an inset in Fig. 1(b) with a size of  $r_0 = 30 \mu\text{m}$ . To observe the emission characteristics, the laser was excited by dc current injection. The output was launched into a fiber with a cone-type input facet at an angle of  $70^\circ$ . The fiber core is spherical with a radius of  $15 \mu\text{m}$ . For measurement, the fiber facet is placed at a distance of approximately  $500 \mu\text{m}$  from the center of the cavity. The launched power is measured using a power meter (Newport 818-IR) connected to a multi-function optical meter (Newport 1835-C), and the spectrum is measured using an optical spectrum analyzer (Agilent 86142B).

We observed that the emission intensity depends on the injection current as shown in Fig. 3. In the figure, we can clearly observe a change in slope at approximately 80 mA, which is the lasing threshold. The slope above 80 mA is steeper than the one below the threshold. This is an evidence of lasing. The slope below the threshold is caused by the highly lossy characteristics of our microcavity laser. The laser was damaged above 100 mA, and therefore, we obtained the slope only up to 95 mA.

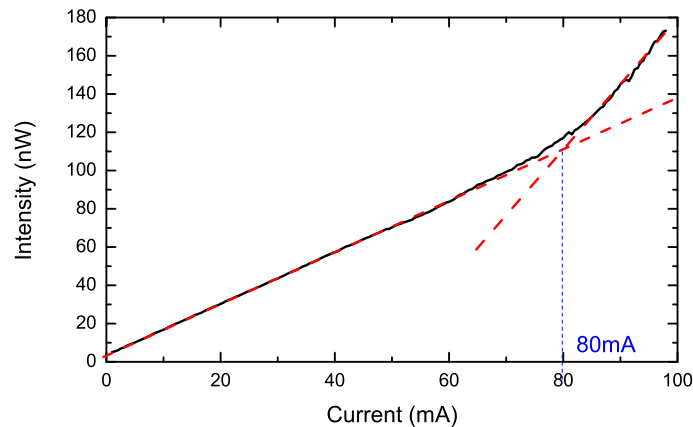


Fig. 3. Output power depending on the injection current; threshold is approximately 80 mA. The output power is measured at  $\theta = 0^\circ$ . Here, the intensity is plotted arbitrarily.

The optical spectra are measured for two cases of injection current: near and far above the threshold. When the current is below the threshold, the laser exhibits no sharp peak in the spectrum. As the current increases, sharp resonance modes begin to appear. When the injection current is 70 mA, various modes are lased in the range 1,570-1,610 nm as shown in Fig. 4(a), which is another evidence of lasing. In the figure, we can observe periodic lasing modes. When the injection current is 95 mA, the lasing mode at approximately 1598.4 nm is dominant and is accompanied by several low power modes, as shown in Fig. 4(b). From the spectrum, we obtain the quality ( $Q$ ) factor of the main lasing mode. Because the  $Q$ -factor of this lasing mode can be measured near the threshold [20, 21], we obtain the linewidth of the lasing mode at 70 mA using the spectrum analyzer, whose resolution is 0.06 nm. Figure 4(c) shows a linewidth of 0.21 nm. From the relationship  $Q = \lambda / \Delta\lambda$ , we obtain a  $Q$ -factor of  $\sim 7,700$ . This relatively

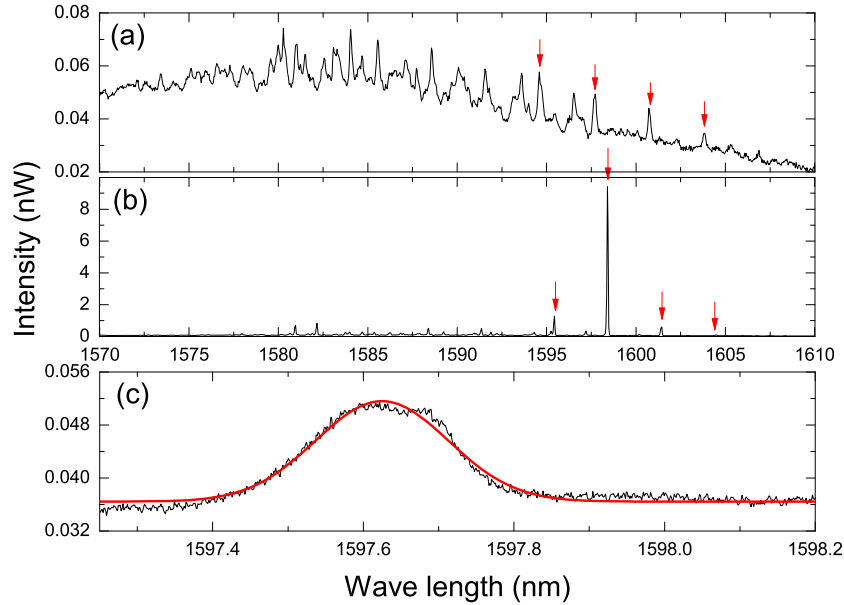


Fig. 4. Optical spectra. (a) Spectrum at 70 mA. The red arrows show a mode group that contains a lasing mode with an average mode spacing of 3.06 nm. (b) Spectrum at 96 mA. (c) Enlarged spectrum of the second peak of the mode group at 70 mA. The red curve is the Gaussian fitting of the spectrum. The linewidth is 0.21 nm.

high  $Q$ -factor is caused by the lasing modes localized on the period-5 unstable periodic orbit, which has an incident angle higher than the critical angle, as shown in Fig. 2.

Further, an angularly distributed FFP is measured at the injection current of 95 mA as shown in Fig. 5. The fiber facet was placed at a distance of  $500\mu\text{m}$  from the center of the cavity and the fiber was rotated. Subsequent peak powers of the main lasing modes were measured. The black and blue lines represent experimentally and ray dynamically obtained FFPs, respectively. The emission intensity is normalized to be unity at the highest intensity angle. The experimental result conforms to the ray dynamical one. The emission direction was confirmed by evaluating five samples. In the figure, the backward emission in the experiment is higher than the one in ray dynamics due to spontaneous emission. The backward emission at 95 mA is lower than the one at 80 mA. This result implies that when the deformation parameter of a cardioid-shaped microcavity laser with reflection symmetry is well adjusted, the laser emits unidirectionally.

To demonstrate the periodic orbit supporting the main lasing mode, the mode spacing was obtained from the mode group involving the main lasing mode. From the spectra in Fig. 4(a) and (b), we obtained the lasing mode group marked by red arrows. The lasing modes in Fig. 4(a) are slightly red-shifted from those in Fig. 4(b) owing to thermal heating. In spite of mode shifting, the mode spacing is maintained. The path length of the periodic orbit, where the lasing modes are localized, is related to the mode spacing by the following equation:

$$L = \frac{\{(\lambda_1 + \lambda_2)/2\}^2}{n_g \Delta\lambda}, \quad (2)$$

where  $L$  is the path length,  $\Delta\lambda$  is the mode spacing between two neighboring lasing modes  $\lambda_1$  and  $\lambda_2$ , and  $n_g$  is the group refractive index. In our measurement, because  $\lambda_1 = 1595.44$  nm,  $\lambda_2 = 1598.40$  nm,  $\lambda_3 = 1601.44$  nm, and  $\lambda_4 = 1604.48$  nm, the average path length is

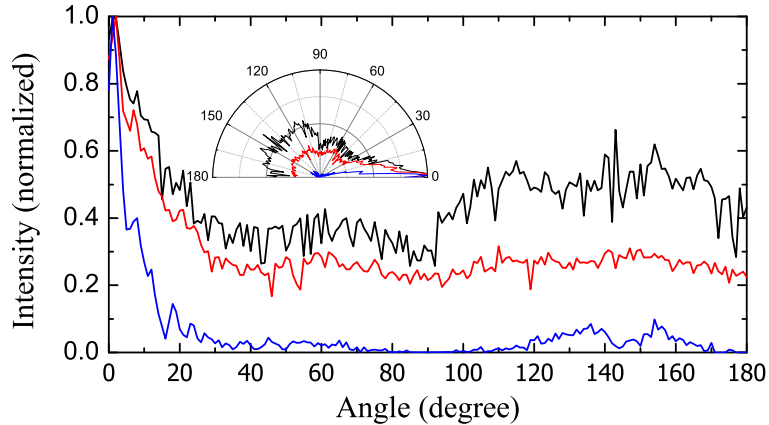


Fig. 5. Experimentally obtained FFPs of the cardioid-shaped microcavity at 80 mA (black) and 95 mA (red). The blue curve is the ray dynamical FFP. The output intensity is normalized to be 1.0 at the maximum intensity.

$L_{avg} \sim 230.87 \mu\text{m}$  for  $n_g = 3.68$  [22]. The path length well coincides with the length of the period-5 periodic orbit, which is  $\sim 233 \mu\text{m}$  for  $R_0 = 30 \mu\text{m}$ . The deviation is approximately 1%. From the spectrum analysis, we confirmed that the lasing modes are localized on the pentagon-type orbit.

#### 4. Conclusion

In conclusion, we have obtained unidirectional emission in a cardioid-shaped microcavity, with which has reflection symmetry. In a ray dynamical calculation, when  $\varepsilon = 0.48$ , the microcavity emits unidirectionally. The period-5 periodic orbit supports unidirectional emission. To confirm this result, we fabricated a laser by using an InGaAsP semiconductor with a size of  $r_0 = 30 \mu\text{m}$ . When the laser was excited by CW current injection, the laser emitted unidirectionally. From the mode spacing in the spectrum, we confirmed that the lasing modes are localized on the period-5 periodic orbit. The experimental results conform to well coincide with the ray dynamical results.

#### Acknowledgments

I-G Lee and S-M Go have made equal contributions as first authors. This research was supported by Basic Science Research Program (Grant No. NRF-2013R1A1A2060846) and High-Tech Convergence Technology Development Program (Grant No. NRF-2014M3C1A3051331) through the National Research Foundation of Korea (NRF) funded by the Ministry of Science, ICT and Future Planning.